AIP | Applied Physics Letters

Monolayer graphene growth on Ni(111) by low temperature chemical vapor deposition

Rafik Addou, Arjun Dahal, Peter Sutter, and Matthias Batzill

Citation: Appl. Phys. Lett. **100**, 021601 (2012); doi: 10.1063/1.3675481
View online: http://dx.doi.org/10.1063/1.3675481
View Table of Contents: http://apl.aip.org/resource/1/APPLAB/v100/i2
Published by the American Institute of Physics.

APPLIED PHYSICS LETTERS **100**, 021601 (2012)

Monolayer graphene growth on Ni(111) by low temperature chemical vapor deposition

Rafik Addou,[1] Arjun Dahal,[1] Peter Sutter,[2] and Matthias Batzill[1,a)]
[1]*Department of Physics, University of South Florida, Tampa, Florida 33620, USA*
[2]*Center for Functional Nanomaterials, Brookhaven National Laboratory, Upton, New York 11973, USA*

(Received 4 November 2011; accepted 12 December 2011; published online 9 January 2012)

In contrast to the commonly employed high temperature chemical vapor deposition growth that leads to multilayer graphene formation by carbon segregation from the bulk, we demonstrate that below 600 °C graphene can be grown in a self-limiting monolayer growth process. Optimum growth is achieved at ∼550 °C. Above this temperature, carbon diffusion into the bulk is limiting the surface growth rate, while at temperatures below ∼500 °C a competing surface carbide phase impedes graphene formation. © *2012 American Institute of Physics*. [doi:10.1063/1.3675481]

Graphene synthesis by chemical vapor deposition (CVD) on late transition metal substrates, such as Cu,[1] Ni,[2] Ru,[3] Ir,[4] or Pt,[5] is a promising approach for the synthesis of large area graphene wafers.[6,7] The low carbon solubility in copper leads to a desirable self-limiting surface growth of graphene,[7,8] while on other materials, including Ni, carbon dissolution into the bulk at typical high growth temperatures of 900 °C can result in carbon re-segregation and multilayer graphene formation upon cooling.[9,10] On copper, the high temperatures needed for graphene growth are close to its melting temperature, resulting in copper sublimation and surface roughening during growth.[11] Furthermore, the weak interaction between graphene and copper causes the formation of multiple graphene-domains with different orientations[12] and therefore twist domain boundaries in graphene cannot be avoided even on single crystalline copper substrates. Nickel has been originally suggested for graphene synthesis[2,13] and would have some advantages over copper if multilayer graphene formation could be avoided. For instance, because of a stronger graphene-metal interaction and better lattice match, graphene is in registry with Ni(111) (Ref. 14) and consequently only one graphene-domain-rotation exists for graphene grown on single crystalline Ni. Therefore, no tilt-grain boundaries are expected after the coalescence of graphene domains to a closed film.[15] Here, we demonstrate by real-time observations in a low energy electron microscope (LEEM) that graphene with large (several tens of μm^2) domains can be grown effectively in *surface growth mode* at relatively low substrate temperatures (∼550 °C) and therefore a similar self-terminating monolayer growth as for copper can be achieved.

We have grown graphene by ultrahigh vacuum (UHV) chemical vapor deposition with ethylene (C_2H_4) as the precursor molecule at a pressure of 10^{-6} Torr. The growth of graphene on the Ni(111) single crystal was monitored with a Elmitec V LEEM and with Auger electron spectroscopy (AES) using a double pass cylindrical mirror analyzer in two separate UHV systems. Figure 1 shows LEEM studies for determining the thermal stability of graphene monolayers on Ni(111). Above 650 °C, the graphene layer starts to disintegrate in agreement with previous electron spectroscopy results.[13,16] This stability temperature of graphene sets an upper limit for the growth temperature of graphene in a surface growth mode on nickel. At low temperatures (<400 °C), a surface carbide phase is formed. Our previous AES studies demonstrated that this surface carbide phase is stable up to ∼480 °C.[13] This carbide phase impedes the nucleation and growth of graphene. Therefore, in this study, we chose three growth-temperatures, 500 °C, 550 °C, and 600 °C, which lie in between the phase stability limits of the surface-carbide and graphene.

Figure 2 shows LEEM images and AES spectra of the surface at different ethylene exposures at 500 °C. LEEM shows the onset of a transformation of the clean Ni(111) surface into a different surface phase for 5-100L exposures. From correlation with AES measurements, we can identify this phase as the ordered monolayer surface carbide previously discussed in detail.[13,17] The first graphene nucleation is observed after increasing the ethylene exposure to 760L. At 500 °C, the growth front of these graphene islands advances at an initial rate of ∼5.5 nm/s. In the LEEM movies, we cannot identify any separation between the advancing graphene grain and the Ni_2C phase. Therefore, it is possible that graphene grows by a direct conversion of the carbide in agreement with previous scanning tunneling microscopy (STM) studies.[18]

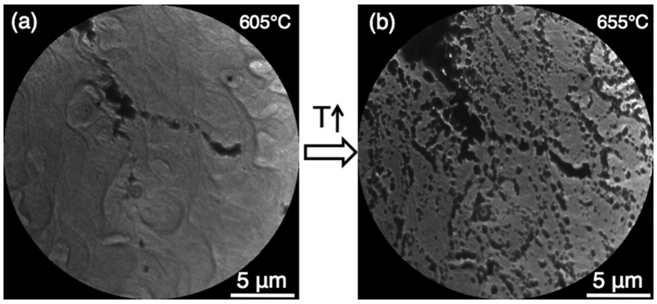

FIG. 1. LEEM images illustrating the thermal stability of monolayer graphene on Ni(111). (a) shows a Ni(111) surface almost entirely covered by graphene (dark areas are uncovered Ni-substrate) at a sample temperature of 605 °C. Upon raising the temperature to 655 °C, the graphene sheet is starting to dissolve as shown in (b).

[a)] Author to whom correspondence should be addressed. Electronic mail: mbatzill@cas.usf.edu.

0003-6951/2012/100(2)/021601/3/$30.00

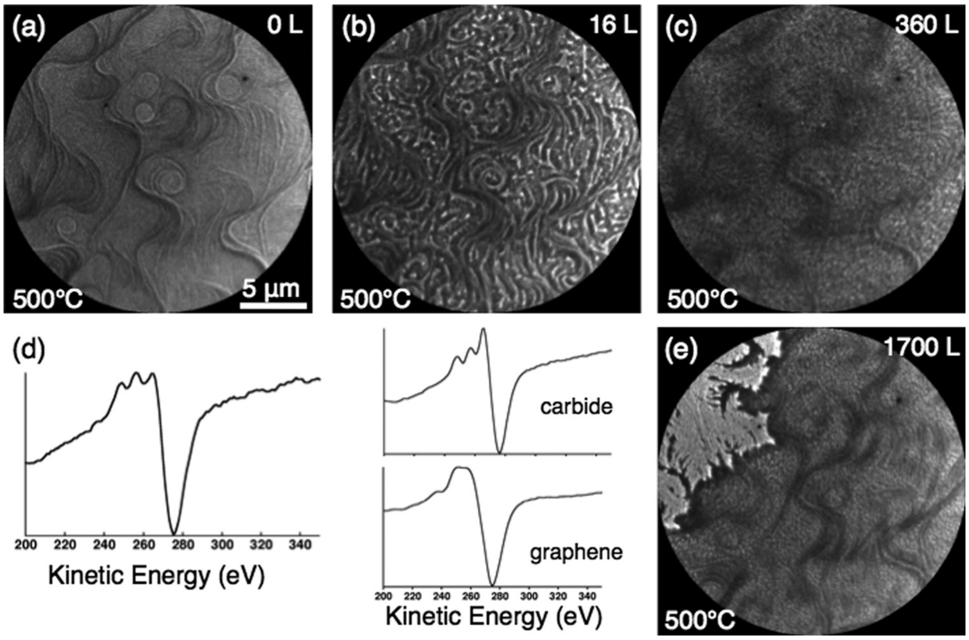

FIG. 2. Surface evolution of Ni(111) exposed to 10^{-6} Torr ethylene at 500 °C. The clean Ni(111) surface is shown in (a). Bright lines correspond to atomic steps on the surface. After exposure to only 16 L ethylene the surface converts initially to a coarse surface carbide (b), which with increasing exposure develops a finer microstructure (c). At even higher exposures, graphene nucleates and grows in a rather fragmented sheet as can be seen in the upper left corner of (e). The presence of both carbide and graphene at this sample temperature is also verified by AES shown in (d). The shape of the C_{KVV} AES spectrum at ~400L exposure is a superposition of the pure-carbide and pure-graphene reference spectra shown on the right in (d).

At 550 °C, the surface dynamics is markedly different. In AES, we do not observe the formation of a well defined carbide signal. Only a weaker C_{KVV} signal is observed, which has, however, some carbide component so that we conclude that only isolated carbide domains or a disordered carbide layer is formed. At 600L exposure graphene nucleates. One difference in the graphene growth at 550 °C is the growth rate of graphene is now ~35 nm/s, i.e., it is about 7 times faster than for graphene growth at 500 °C. A second important difference is that a zone, about 3-4 μm wide, is observed in front of the growing graphene (see Fig. 3(b)). This zone indicates the formation of a carbon-denuded zone in front of the graphene, which is consistent with a carbon concentration gradient surrounding the graphene islands. This observation demonstrates that at this temperature the graphene is not in direct contact with a carbon-dense (carbide) phase and therefore graphene grows in a similar fashion as on other transition metals, i.e., by carbon attachment to the free graphene edge. Importantly, the carbon denuded zone indicates that graphene growth is dominated by surface diffusion and not by bulk carbon re-segregation. Carbon surface diffusion as the dominating growth mechanism is also further supported by the observation that the growth speed of graphene grains slows down once two grains approach each other, i.e., the growth rate depends on the available surface area for carbon to form by dehydrogenation of ethylene. The reduced growth speed also leads to gaps between graphene grains that take longer to be filled in. These gaps can be seen in large-scale LEEM images such as the one shown in Fig. 3(c). From this large scale image, a typical grain diameter of the order of ~40 μm is apparent.

Increasing the temperature further to 600 °C causes additional changes: (i) even less carbide formation is observed in AES and the first significant carbon signal is that of graphene, (ii) graphene nucleation requires a 4 times higher ethylene exposure, (iii) the denuded zone in front of the graphene edge is 3-4 times wider, i.e., 10-15 μm; this is clearly seen in Figure 3(d), and (iv) the growth rate of graphene is only about 1/7 that at 550 °C, i.e., ~4.8 nm/s.

Clearly the growth of graphene on Ni in a surface-growth mode is fastest around 550 °C and considerably slower at higher and lower temperatures. Some general considerations may explain this maximum in the growth rate. The decreasing growth rate at higher temperatures is explained by the competition between carbon surface diffusion towards the graphene growth front and the loss of surface carbon by diffusion into the bulk. In a simple model of

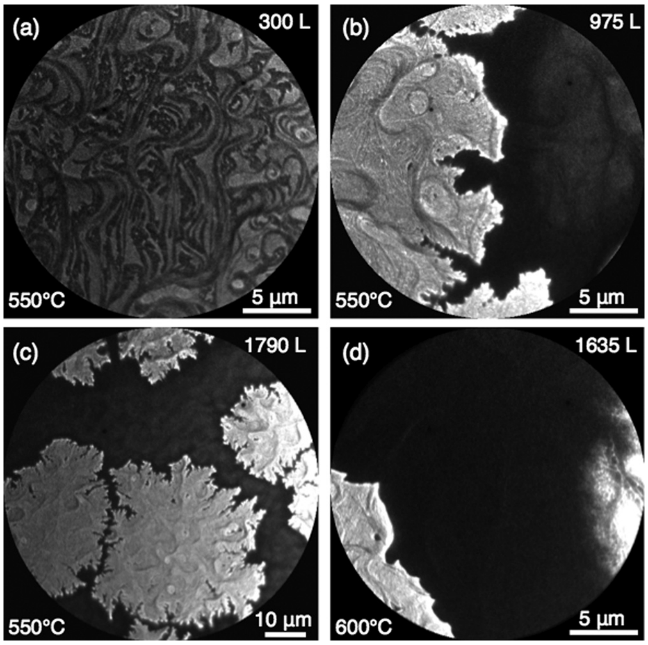

FIG. 3. LEEM images of surface structures at 550 °C (a)-(c) and 600 °C (d) for different ethylene exposures as indicated in the upper right corner of each image. Exposure to ethylene at 550 °C results in the formation of isolated carbide domains (a) for low ethylene exposure. Graphene growth is accompanied by formation of dark-contrast area in front of the graphene-edge (b). This zone is interpreted as a carbon denuded zone. A similar, but much wider zone, is formed at a growth temperature of 600 °C, evident in (d). A large area (77 μm field of view) is shown in (c) for 550 °C growth temperature. This view enables to assess the average graphene domain sizes before coalescence.

thermally activated processes with activation barriers E_s and E_b for surface and bulk diffusion, respectively, the *ratio of bulk to surface diffusion* increases exponentially with temperature as exp $(E_s - E_b/kT)$ (assuming the same pre-exponential factor for both diffusion processes.) Additional factors for a decreasing growth rate may be a reduced sticking and decomposition of ethylene. However, such strong temperature dependence of the sticking coefficient is unlikely for identical surfaces. This may be different at the low temperature limit of 500 °C, where the surface is transformed into a surface carbide. Carbides are expected to have a reduced reactivity towards ethylene compared with pure Ni. Therefore, the rapid formation of a full monolayer of carbide at 500 °C may reduce the formation of activated carbon. An alternative explanation for the drop in the growth rate at 500 °C is that the growth mechanism for graphene is substantially different in the presence of the surface carbide.[18] At 550 °C and 600 °C, graphene grows on pure Ni, and the growth mode is, therefore, similar to that reported for other transition metals, i.e., by attachment of carbon or carbon-clusters to the free-edges of the graphene islands.[19,20]

In conclusion, our *in situ* microscopy experiments on the CVD growth of graphene on Ni(111) show that self-limiting monolayer graphene growth can be obtained on nickel substrates if the growth temperatures are adjusted to below the graphene phase-stability temperature of ∼650 °C. The optimum growth temperature is close to 550 °C. This optimum growth temperature is determined by the interplay between the formation of a surface carbide, which limits the growth of high quality graphene at low temperature (below 500 °C) and carbon dissolution into the bulk, which limits growth at high temperatures (above 600 °C).

The USF group acknowledges financial support from the Office of Naval Research under Award No. N00014-10-1-0668. This research has been carried out in part at the Center for Functional Nanomaterials, Brookhaven National Laboratory, which is supported by the U.S. Department of Energy, Office of Basic Energy Sciences, under Contract No. DE-AC02-98CH10886.

[1] X. Li, C. W. Magnuson, A. Venugopal, R. M. Tromp, J. B. Hannon, E. M. Vogel, L. Colombo, and R. S. Ruoff, J. Am. Chem. Soc. **133**, 2816 (2011).
[2] A. Reina, X. Jia, J. Ho, D. Nezich, H. Son, V. Bulovic, M. S. Dresselhaus, and J. Kong, Nano Lett. **9**, 30 (2008).
[3] P. W. Sutter, J. I. Flege, and E. A. Sutter, Nature Mater. **7**, 406 (2008).
[4] J. Coraux, A. T. N'Diaye, C. Busse, and T. Michely, Nano Lett. **8**, 565 (2008).
[5] P. Sutter, J. T. Sadowski, and E. Sutter, Phys. Rev. B **80**, 245411 (2009).
[6] S. Bae, H. Kim, Y. Lee, X. Xu, J. S. Park, Y. Zheng, J. Balakrishnan, T. Lei, H. R. Kim, Y. I. Song *et al.*, Nat. Nanotechnol. **5**, 574 (2010).
[7] X. Li, W. Cai, L. Colombo, and R. S. Ruoff, Nano Lett. **9**, 4268 (2009).
[8] K. S. Kim, Y. Zhao, H. Jang, S. Y. Lee, J. M. Kim, K. S. Kim, J. H. Ahn, P. Kim, J. Y. Choi, and B. H. Hong, Nature (London) **457**, 706 (2009).
[9] J. C. Shelton, H. R. Patil, and J. M. Blakely, Surf. Sci. **43**, 493 (1974).
[10] A. Reina, S. Thiele, X. Jia, S. Bhaviripudi, M. S. Dresselhaus, J. A. Schaefer, and J. Kong, Nano Res. **2**, 509 (2009).
[11] J. W. Wofford, S. Nie, K. F. McCarty, N. C. Bartelt, and O. D. Dubon, Nano Lett. **10**, 4890 (2010).
[12] L. Gao, J. R. Guest, and N. P. Guisinger, Nano Lett. **10**, 3512 (2010).
[13] J. Lahiri, T. S. Miller, A. J. Ross, L. Adamska, I. I. Oleynik, and M. Batzill, New J. Phys. **13**, 025001 (2011).
[14] Y. Gamo, A. Nagashima, M. Wakabayashi, M. Terai, and C. Oshima, Surf. Sci. **374**, 61 (1997).
[15] J. Lahiri, Y. Lin, P. Bozkurt, I. I. Oleynik, and M. Batzill, Nat. Nanotechnol. **5**, 326 (2010).
[16] A. Grüneis, K. Kummer, and D. V. Vyalikh, New J. Phys. **11**, 073050 (2009).
[17] J. J. McCarroll, T. Edmonds, and R. C. Pitkethly, Nature (London) **223**, 1260 (1969).
[18] J. Lahiri, T. Miller, L. Adamska, I. I. Oleynik, and M. Batzill, Nano Lett. **11**, 518 (2011).
[19] E. Loginova, N. C. Bartelt, P. J. Feibelman, and K. F. McCarty, New J. Phys. **11**, 063046 (2009).
[20] E. Loginova, N. C. Bartelt, P. J. Feibelman, and K. F. McCarty, New J. Phys. **10**, 093026 (2008).